Journal of Structural Geology 33 (2011) 1394–1405

Contents lists available at ScienceDirect

Journal of Structural Geology

journal homepage: www.elsevier.com/locate/jsg

Puzzles and the maximum-effective-moment (MEM) criterion in structural geology

Yadong Zheng [a,*], Jinjiang Zhang [a], Tao Wang [b]

[a] The Key Laboratory of Orogenic Belts and Crustal Evolution, Ministry of Education, School of Earth and Space Sciences, Peking University, Beijing 100871, China
[b] Institute of Geology, Chinese Academy of Geological Sciences, Beijing 100037, China

ARTICLE INFO

Article history:
Received 19 May 2010
Received in revised form
10 June 2011
Accepted 17 June 2011
Available online 29 June 2011

Keywords:
MEM-Criterion
Low-angle normal fault
High-angle reverse fault
Wide-open V-shaped conjugate strike-slip faults
Strain-rate

ABSTRACT

The essential difference in the formation between conjugate brittle shear fractures and ductile shear zones is that the intersection angle of conjugate faults in the contractional quadrants in the former is acute (usually ~60°) and obtuse (usually 110°) in the latter. The Mohr-Coulomb failure criterion is an experimentally validated empirical relationship, which structural geologists use to interpret the stress directions based on the orientation of the brittle shear fractures. However, a simple application of this criterion assuming that the principal stresses are vertical or horizontal throughout the crust fails to explain crustal scale low-angle normal faults, high-angle reverse faults and certain types of conjugate strike-slip faults that have intersection angles in the compressional quadrants greater than 90°.

Although the Maximum-Effective-Moment (MEM) criterion has been used to analyze structures in several natural cases and obtained some new evidence in nature and experiments, it is not yet commonly used to interpret non-Mohr-Coulomb features widely distributed in the crust. It is important to review the MEM criterion and its implications for explaining the formation mechanism of naturally occurring faults and shear zones. Behavior of a rock depends on its mechanical properties; the latter in turn depends on pressure and temperature conditions related to crustal depth and strain rates.

Conjugate fractures with obtuse angles, ca. 110°, in the contractional direction at different scales and at different crustal levels are consistent with the prediction of the MEM criterion and suggest deformation at low strain rates. Thus, strain-rate clearly plays an important role in the style of crustal deformation and the many observed departures from the Mohr-Coulomb failure criterion.

1. Introduction

Recognition of low-angle normal faults (i.e. extensional detachment faults) in Cordilleran metamorphic core complexes western North America in the early 1980's (e.g. Wernicke, 1981) were a significant discovery in the history of structural geology. Similar faults were subsequently reported elsewhere in the world. The occurrence of these low-angle faults is not compatible with the Mohr-Coulomb criterion. Based on the criterion and the assumption that the principal stresses are vertical and horizontal through the crust, Anderson (1951) predicted that normal faults dip at angles more than 45°, whereas thrusts dip at angles less than 45°.

A brief summary of structures in the Earth's crust was given by Ramsay (1980): low-angle thrusts in the brittle upper part of the continental crust and high-angle reverse ductile shear zones in the ductile middle–lower part of the crust can form in contractional regimes, and high-angle normal faults in the brittle upper crust and low-angle normal ductile shear zones in the ductile mid-lower crust can form in extensional regimes. The formation of low-angle thrusts and high-angle normal faults in brittle domains can be reasonably explained with the Mohr-Coulomb criterion, because the criterion predicts the orientation of fractures as inclined to the maximum principal compressive stress (σ_1) at an angle less than 45°, i.e., the conjugate angle of fractures on the σ_1 sides is always acute. However, problems with the mechanical origin of low-angle normal faults and high-angle reverse faults have become a focus of studies in the past three decades. These problems are addressed in this paper.

A major feature shared among low-angle normal fault systems, high-angle reverse faults and V-shaped conjugate strike-slip fault systems (Yin, 2010) is their conjugate obtuse angle (~110°) facing the shortening direction. How to explain the formation of such fractures? Most geologists tend to believe that a progressive contractional process causes the acute angle to switch into an obtuse one (e.g. Mitra, 1979; Ramsay and Huber, 1987; Carreras

* Corresponding author.
E-mail address: ydzheng@pku.edu.cn (Y. Zheng).

0191-8141/$ – see front matter © 2011 Elsevier Ltd. All rights reserved.
doi:10.1016/j.jsg.2011.06.004

et al., 2010). If this explanation were correct, the conjugate angle of ductile shear zones would be acute or 90° at the beginning of fault formation and then keep increase with subsequent flattening until it approaches 180°. Conjugate angles observed in nature and experiments, however, are usually ~110° (Zheng et al., 2004, 2006). If the conjugate angles were initially 90° and turned into 110° with progressive deformation, then according to Harker's formula for plane-deformation (cf. Ramsay, 1980) R_s = tan45°/tan35.3°, the negative extension ($-\epsilon$) needed would be −17%. If 3D-strain is involved the strain needed would be even higher. However, experiments on phyllite conducted by Paterson and Weiss (1966) demonstrated that conjugate kink-bands with an initial angle of ~110° in the direction of the maximum compression appeared at shortening of ~10%, and the angle did not change with increased strains to 50%. In experiments on single quartz-crystal deformation, the observed conjugate angle at a shortening of 26% was 110° (Fig. 2A; Vernooij et al., 2006); about the same shortening has appeared in natural deformation (Fig. 2E). A study of the angles between conjugate shear bands by Kurz and Northrup (2008) show that all in both high-strained and low-strained rocks, fall in the range predicted by the MEM criterion (the four vertical lines in the shadow of Fig. 1) and that the angle of 110° does not increase with progressive strain (Zheng et al., 2009a,b). These diverse observations of stable angle are obviously not compatible with progressive flattening theories.

Waterston (1999) re-evaluated the Becker's theory (1893) and proposed the zero-extension theory, which suggested that formation of ductile shear zones follow the zero-extension directions of an infinitesimal strain ellipsoid. The conjugate angle predicted by Watterson is 90° for a plane strain and 109.4° for uniaxial shortening. Although the value of the latter does correspond well with observations in nature and laboratories, it is unfortunately only applicable to uniaxial shortening where the locus of zero-extension directions is a pair of conical surfaces rather than conjugate planar shear zones as observed in nature. It is quite surprising, yet very interesting that the result under uniaxial extensional cases that is opposite to that given by slip-line theory of plasticity: the maximum principal stress axis bisects the *acute* angle (180°−109.4° = 70.6°) rather the obtuse one (109.4°) of conjugate slip-line sets (Hill, 1950). The strange 109.4°, therefore, is derived from the three different approaches that give the three different predictions as summed up as follows:

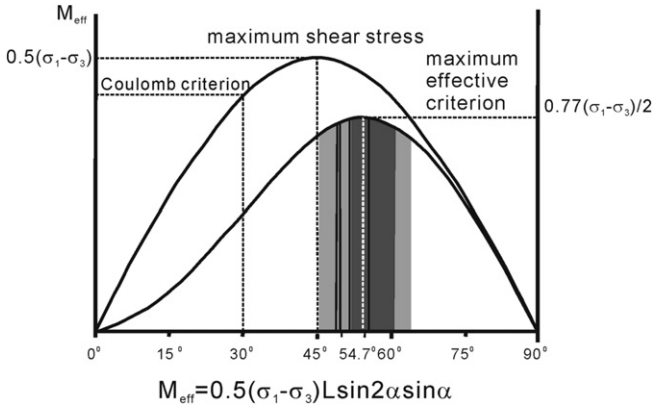

Fig. 1. Coulomb criterion and the maximum effective moment criterion (Based on Zheng et al., 2004): (σ_1−σ_3) - yield strength of the material; α-the angle between σ_1 and the normal to shear bands/zones; *L*-unit length; shadow area in grey covering all the data available and shadow area in dark-grey covering all the data with a distinct yield stress provided by Gómez-Rivas (2008). The four vertical lines represent the four conjugate angles measured by Kurz and Northrup (2008).

1) the zero-extension theory, predicting a pair of conical surfaces with 109.4° in shortening direction, which is only applicable to uniaxial shortening;
2) slip-line theory of plasticity, predicting a pair of conical surfaces with 109.4° in extension direction for uniaxial extension, which is incompatible with observations in nature and laboratories (Fig. 1);
3) the MEM criterion with the unit-length in the σ-1 direction, predicting conjugate shear zones with 109.4° in shortening direction, which is well correspond with observations in nature and laboratories (Fig. 1). Obviously, neither of them but 3) are suitable for the explanation of the formation of low-angle normal faults, high-angle reverse faults and V-shaped conjugate strike-slip faults. In a case-study, Zheng et al. (2004) argued that extensional crenulation cleavages (eccs) controlled by the orientations of the MEM may turn into large-scale low-angle normal faults through strain-softening and strain-localization.

Although the MEM criterion has been used to explain conjugate shear zones and kink-bands in several recent publications (e.g., Neves et al., 2005; Marshak et al., 2006; Zheng et al., 2006; Guo et al., 2006; Yang et al., 2007; King et al., 2008; Fowler and Osman, 2009; Zhang et al., 2010), the criterion is not yet familiar to most geologists. As an example of this, Gomez-Rivas (2008) states that: "*The dihedral angles between conjugate fracture sets are always higher than 105° and the principal compression stress σ_1 is always parallel to the obtuse bisector between these sets … Therefore, the angle ξ between σ_1 and fractures does not fit any of the classical failure criteria and differs from the observations of any authors in brittle anisotropic rocks.*" If the author had known of the published MEM criterion, he would not have said so. In terms of the MEM criterion, problems and related puzzles in structural geology such as the origins of low-angle normal faults, high-angle reverse faults and so-called "V-shaped conjugate faults" by Yin (2010) are not difficult to resolve. The latter, V-shaped conjugate systems, are widespread in central Tibet, the eastern Alps, Western Turkey, eastern Afghanistan, Western Mongolian, Southeast Asia, and the Gulf of Thailand (Yin and Taylor, in press, and references therein). Since these obtuse angle *V-shaped conjugate faults* can be confused with normal conjugate faults with acute angles in the σ_1-direction, as predicted by the Mohr-Coulomb criterion, we suggest adding the adjective wide-*open* to this type of conjugate faults.

Wide-Open V-shaped conjugate strike-slip faults in Asia are typically related to extrusion tectonics (Tapponnier et al., 1982; Peltzer and Tapponnier, 1988). However, because the geometry of the wide-open V-shaped conjugate strike-slip fault systems departs greatly from fault orientations predicted either by the Mohr-Coulomb fracture criterion or the slip-line theory of plasticity (Hill, 1950), it requires, as Yin realized (2010; Yin and Taylor, 2011), "an unknown mechanism" to explain it. Given the fact that the MEM criterion is not yet commonly used, a review or synthesis is needed. The purpose of this paper is to provide a brief summary of the MEM criterion and some new observations from field and laboratory that can be regarded as solid evidence in support of the criterion. The latter can improve our understanding of rock deformational behavior under varying physical conditions.

2. MEM criterion

Shear bands (White, 1979; White et al., 1980), extensional crenulation cleavages (eccs; Platt, 1979) and kink bands (e.g. Anderson, 1964) are the results of localization of rock-deformation under stress. A basic feature they share is the rotation or deflection of preexistent planar elements (bedding, cleavage, schistosity, mylonitic foliation or man-made marker) in the deformation zones.

The rotation must be directly related to a moment and, no doubt, the orientations of the maximum moment are most favorable for these deformation zones to form. Using the moment approach, the MEM Criterion is proposed for ductile deformation (Zheng et al., 2004). The criterion is mathematically expressed as:

$$M_{eff} = \frac{1}{2}(\sigma_1 - \sigma_3)L\sin 2\alpha \sin \alpha \quad (1)$$

where $(\sigma_1 - \sigma_3)$ represents the yield strength of a material or rock, L is the unit length in the σ_1 direction, and α is the angle between σ_1 and a certain plane. Its graphical expression is shown in Fig. 1; this illustrates that the moment reaches its maximum value when α is $\pm 54.7^\circ$, which is the most favorable angle for forming ductile shear zones and implies that deformation zones tend to appear in pairs with a conjugate angle of 2α, 109.4° facing to σ_1.

The gray shadow area in Fig. 1 shows data available from natural and experimental observations; the range in dark gray covers all of the experimental data provided by Gómez-Rivas (2008). The four vertical lines represent the four natural conjugate angles measured by Kurz and Northrup (2008). All of the data from various materials (homogeneous or heterogeneous, isotropic or anisotropic) and at variable scales confirm the validity of the MEM criterion.

It is necessary to point out that if taking the unit-length in the σ_3 – direction, the maximum value of M_{eff} will appear in the directions of $\pm 35.3^\circ$ to the σ_1 – direction. The conjugate angle predicted in this way should be 70.6°, which is similar to the prediction of the slip-line theory of plasticity for uniaxial extensional cases. Although this result is also derived from mathematics, the predicted orientation with respect to σ_1 departs greatly from observations in nature and experiments (Fig. 1) and is, therefore, invalid.

Major implications of the MEM criterion for physics are as follows.

1) Where there is a differential stress, there are maximum moment orientations. Once the differential stress reaches the yield-strength of the material involved, the shear zones will develop in one or both of the two orientations and the maximum moment becomes the effective one. No shear zones can nucleate when the differential stress is less than the yield-strength of the material in certain deformation circumstances.
2) No matter what material is involved—whether homogeneous or heterogeneous, isotropic or anisotropic, and regardless of crystallographic orientations—ductile shear zones preferably develop parallel to the MEM orientations. The initial conjugate angle of 109.4° in the σ_1-direction is therefore material-invariant and probably does not increase with progressive strain until the related strain reaches ~50% (Paterson and Weiss, 1966).
3) Since no limitations in scale in the range 10^{-7}–10^{8} m (See Section 3) for the MEM criterion, the angle of 109.4° is scale-invariant;
4) Due to the lever-effect, deformation in the MEM orientations is more energy-saving than in other orientations predicted by slip-line theory, or the Mohr-Coulomb criterion, or the zero-extension theory (Watterson, 1999).

3. Typical cases

3.1. Case 1

An excellent experimental study by Vernooij et al. (2006) on ductilely deformed single quartz-crystals reveals that conjugate shear bands form at an obtuse angle of 109°–110° when the crystal is uniaxially compressed parallel to the crystallographic c-axis at 800 °C, at a confining pressure of 1.2 GPa, and an approximately strain rate of 1.1×10^{-6} S^{-1} with its bulk strain reached at ~26% (Fig. 2A). These authors, however, suggest that the shear zones appear to develop along planar microcracks oriented parallel to crystallographic rhomb planes. If this explanation were correct, the angle between c-axis and the shear zones would be 38°13′ rather than ~55°. In reality, there are no crystallographic planes that are parallel to the observed shear bands. It is interesting that a similar situation occurs in natural deformed cordierite as reported by Kruhl et al. (2007). There are also no crystallographic planes in this orthorhombic mineral that are parallel to the shear bands.

3.2. Case 2

A micro-scale example is shown in Fig. 2B where the discrete features are narrow bands that deflect the cleavage of the mica-fish in opposite ways. The conjugate angle between them is 109° in the shortening direction, which is normal to the mylonitic foliation in the Hohhot metamorphic core complex, Inner Mongolia, China (Davis et al., 2002).

3.3. Case 3

Half-natural and half-artificial conjugate ductile shear zones, probably produced at the lowest strain rate available in "experiments" are present in a pillar of shaly sylvinite at a depth of ca. 1 km that sustains the roof of the Boulby Mine, Cleveland, England; the two yield zones cut across each other and displace in a normal sense a set of vertical grooves made by an excavator shovel (Fig. 2C). The upper and lower conjugate angles of 110° and 109°, respectively are reported by Waterston (1999) and regarded as evidence for the zero-extension theory. However, the conjugate angle of 109.4°, predicted by Watterson is for uniaxial shortening in which the locus of zero-extension directions should be a conical surface. In contrast, the pair of planes in the sylvinite pillar with an obtuse angle of 109–110° is exactly what is predicted by the MEM criterion.

3.4. Case 4

Large-scale examples of conjugate shear zones are reported by Park (1981) in granite–greenstone terrain of the Western Superior Province, Canada. As shown in Fig. 2D, the dextral and sinistral sets of ductile shear zones form a conjugate system with an obtuse angle of ~110° in the shortening direction.

3.5. Case 5

A submicroscale example of obtuse conjugate-angles is shown in Fig. 2E (courtesy of Yan Sun; Sun et al., 2008), where the shortening direction bisects the obtuse angle (110°) of the discrete conjugate features in the fault-gouge of the active Haiyang fault, Shandong province, China. The ratio of the strain ellipse (R_s) is 1.73 and corresponds to a negative extension of −26.7%, which is coincidently about the same as the experiment on single quartz-crystal in Case 1 and implies a large-strain deformation.

3.6. Case 6

Outcrop-scale, wide-open conjugate faults deflect and truncate the slaty cleavage of Carboniferous slate in the Nujiang Valley, Yunnan Province, China (Fig. 2F). The angle is ~110° in the EW contractional direction between the vertical NNW-striking right-slip and NNE-striking left-slip fault sets.

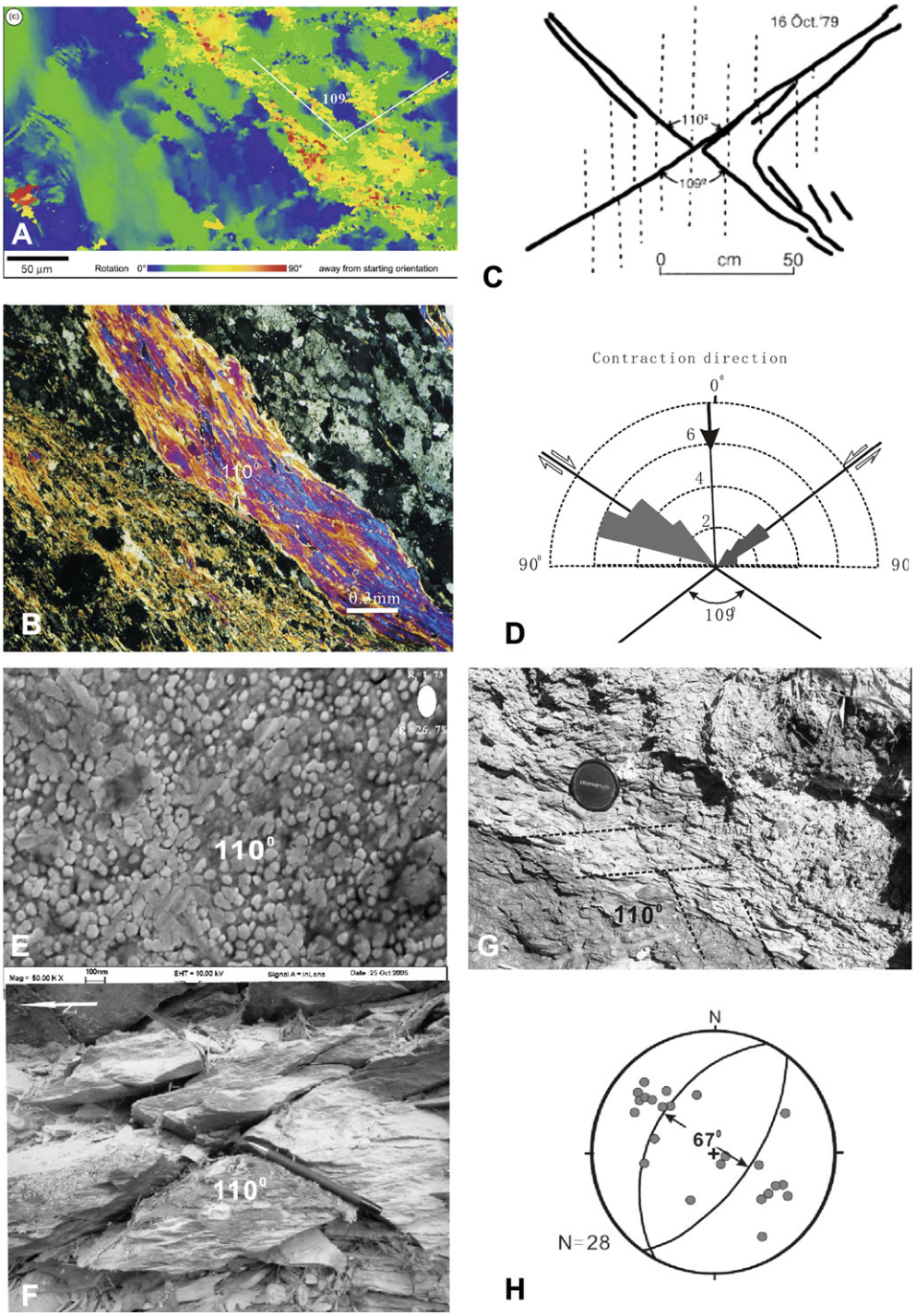

Fig. 2. Examples at various scales and structural levels exhibit the conjugate angle of ~110° between shear bands or zones: (A) micro-scale conjugate shear bands (Vernooij et al., 2007); (B) micro-scale conjugate extensional shear bands in the Hohhot MCC, Inner Mongolia (Zheng et al., 2004); (C) conjugate yield zones in a pillar of shaly sylvinite at a depth of ~1 km in the Boulby mine, Cleveland, England (Watterson, 1999); (D) regional-scale conjugate shear zones in the Western Superior Province, Canada (Park, 1981); (E) conjugate discrete features the fault-gouge of the active Haiyang fault, Shandong province, China (Sun et al., 2008); the ratio of strain ellipse (R_s) is 1.73 and corresponds to a shortening of 26.7%; (F) outcrop-scale conjugate faults with ~110° in the contractional direction that deflect and truncate the slaty cleavage of Carboniferous slate in the Nujiang Valley, China; (G) small-scale conjugate fractures with ~110° in the contractional direction in the gouge zone of the Louzidian detachment fault (eastern Inner Mongolia, China); (H) conjugate deformation bands in argillaceous sediments in the toe of the Nankai accretionary prism in Japan (Ujiie et al., 2004); (I) lozenges surrounded by a conjugate fracture network in a road-cut in Proterozoic phyllite, Changshan Island, China; (K) a close-view of (I) a quartz-vein is located in the positions about the bisector of the obtuse sectors and implies the contraction direction; (J) conjugate normal faults in Neo-Proterozoic non-metamorphic tillite; lineations in the confluence region are closely parallel to the intersection line of the shear zone planes; (K) lineations are sub-parallel to the intersection line of the conjugate normal ductile fractures in the footwall of the Hefangkou detachment, Yunmengshan metamorphic core complex (Davis et al., 1996).

Fig. 2. (*continued*).

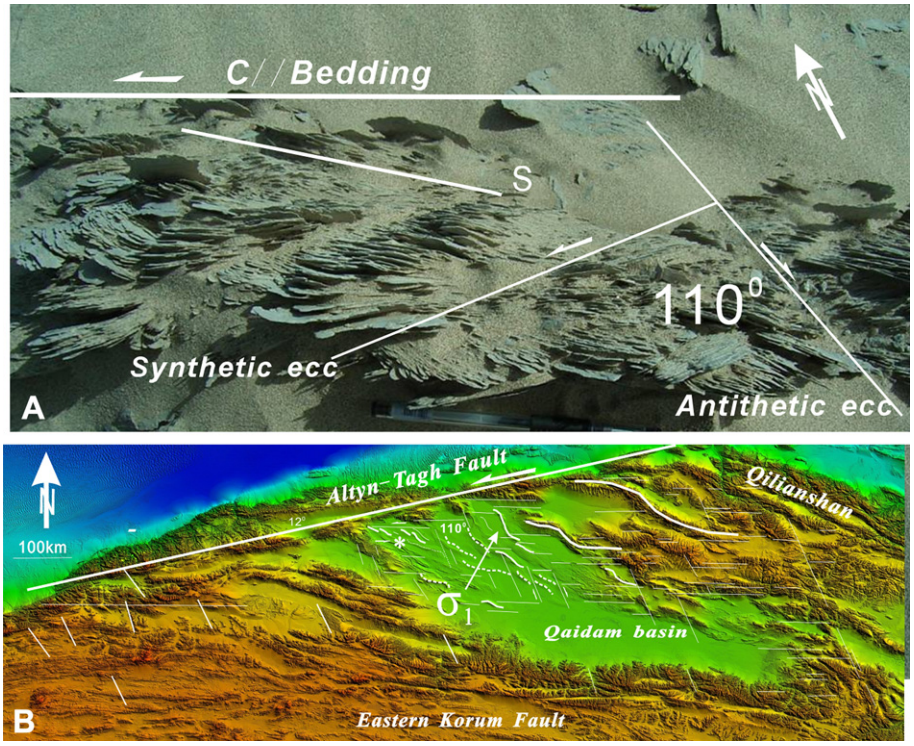

Fig. 3. (A) A downward view of outcrop-scale conjugate ecc sets with ~110° in the shortening direction in a special kind of "schist" in Pliocene non-metamorphosed siltstone located at * of Fig. 3B; (B) two sets of strike-slip faults in the Qaidam Basin, China; the E-W-striking sinistral set has deflected and truncated the Pliocene WNW-trending large-scale kink-zones in an anti-sigmoid pattern (shown in solid lines), whereas the NNW-striking produced the kink-zones' sigmoid pattern (shown in dash-lines). Note that the large-scale S/C fabrics in and adjacent to the Altyn-Tagh sinistral strike-slip fault.

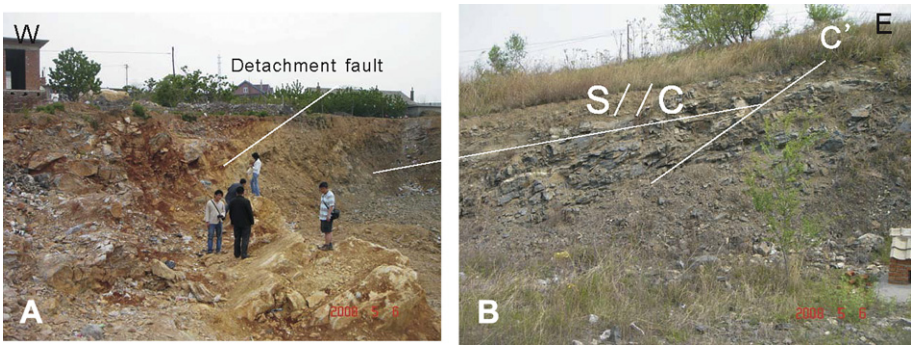

Fig. 4. The Jinzhou extensional detachment fault lies parallel to the spaced C′-foliation in the underlying chloritic mylonitic rocks and truncates the penetrative mylonitic foliation; Liaoning peninsula, China.

3.7. Case 7

Small-scale, wide-open conjugate fractures occurred in the gouge zone in the Louzidian detachment fault of the eastern Inner Mongolia Autonomous Region, China (Wang et al., 2007) and displaced its color bands. The angle between them is ~110° in the contractional direction (Fig. 2G). The S/C fabrics are similar to those of the coseismic shear zone of the 2008 M_w 7.9 Wenchuan earthquake (China) reported by Lin et al. (2010) and imply a ductile behavior of the gouge.

3.8. Case 8

Roughly planar microscopic bands that typically develop in argillaceous sediments at the toe of accretionary prisms are called 'deformation bands'. They are present, for example, in the Nankai accretionary margin in Japan where the Philippine Sea plate is being subducted to the NW at a rate of 4 cm/yr (Ujiie et al., 2004). The bedding in the prism as a whole is sub-horizontal, whereas the bedding and layered silicate minerals in the deformation zones are sub-vertical. The average angle between the conjugate deformation zones in a horizontal direction is 113° (Fig. 2H), which implies that the reverse deformation zones result from lateral contraction related to plate convergence. Ujiie et al. (2004) explained the high-angle reverse deformation zones using Ramsay's (1980) hypothesis in which the angle between compactive brittle–ductile shear zones and σ_1 could be greater than 45°. As mentioned before, however, the theory of compaction fails to explain the quite stable angle of 110°; no problem is raised by the observation that the ~113° conjugate angle reported in the accretionary prism is 3° more than that predicted by the MEM criterion.

3.9. Case 9

Well-exposed wide-open conjugate fracture networks (Fig. 2I) are composed of less deformed lozenges surrounded by anastomosing shear zones in Proterozoic phyllite on the north-wall of a road-cut, Changshan Island, Liaoning Province, China. Subvertial quartz-veins bisect the obtuse sectors and serve to define the contraction direction (Fig. 2J).

3.10. Case 10

Outcrop-scale, wide-open conjugate normal faults occur in Neo-Proterozoic non-metamorphic tillite in the Three Gorges region (Fig. 2k). The conjugate normal faults deflect and truncate bedding in the tillite. The angle between them is ~110° in the contractional direction. As conjugate faults may move synchronously to form an area of high strain near the intersection (Peacock, 1991; Odonne and Massonnat, 1992), the two shear zones meet at the confluence. Rocks in that region are highly strained (probably >50%).

Note that lineations the confluence region are closely parallel to the intersection line of the shear zone planes as described by Ramsay and Allison (1979) and Carreras et al. (2004). Such a situation seems not uncommon in nature as also shown in Fig. 2I where the lineations are sub-parallel to the intersection of the conjugate normal ductile fractures below the detachment of the Yunmengshan metamorphic core complex (Davis et al., 1996). Lineation normal to the XZ-plane implies a mass movement of materials out of the XZ plane; the incompatibility problems arise from simultaneously shearing of conjugate shear zones (Ramsay and Huber, 1987) may be resolved in this way.

3.11. Case 11

There are two sets of strike-slip faults in the Qaidam Basin of China (Fig. 3B). The E-W-striking sinistral set deflects and truncates the Pliocene sub-vertical strata of WNW-trending large-scale kink-zones in an anti-sigmoid pattern and the NNW-trending set made the strata as sigmoid pattern. The dextral features cut sinistral ones and vice versa. These deflections imply that the rocks had experienced quite a large strain before the faults developed and the conjugate angle of ~110° further confirms that these faults belong to ductile features.

3.12. Case 12

MEM angular relationships are observed on Qaidam basin outcrop-scale structures shown in Fig. 3A, where conjugate ecc sets with 110° in the shortening direction are present in Pliocene siltstone with large crystals of gypsum up to 20 cm in length formed by recrystallization and containing numerous silt-grain inclusions. At this locality (* in Fig. 3B on the north-limb of the Oil–Spring culmination in the Qaidam Basin, China; Zheng et al., 2006). the vertical bedding and fabric defined by oriented gypsum crystals constitute an S/C-style relationship; the acute S to C angle of ~12° indicates sinistral shearing. The schistosity is deflected and truncated by the conjugate ecc sets. As usual, the synthetic eccs or C's (Berthe et al., 1979) are much better developed than antithetic ones (White, 1979; White et al., 1980; Zheng et al., 2004). The gypsum crystals appear to have formed at low strain-rates and at very shallow levels.

Clearly, all these observations from nature and experiments provide diverse and convincing evidence for the applicability of the MEM Criterion.

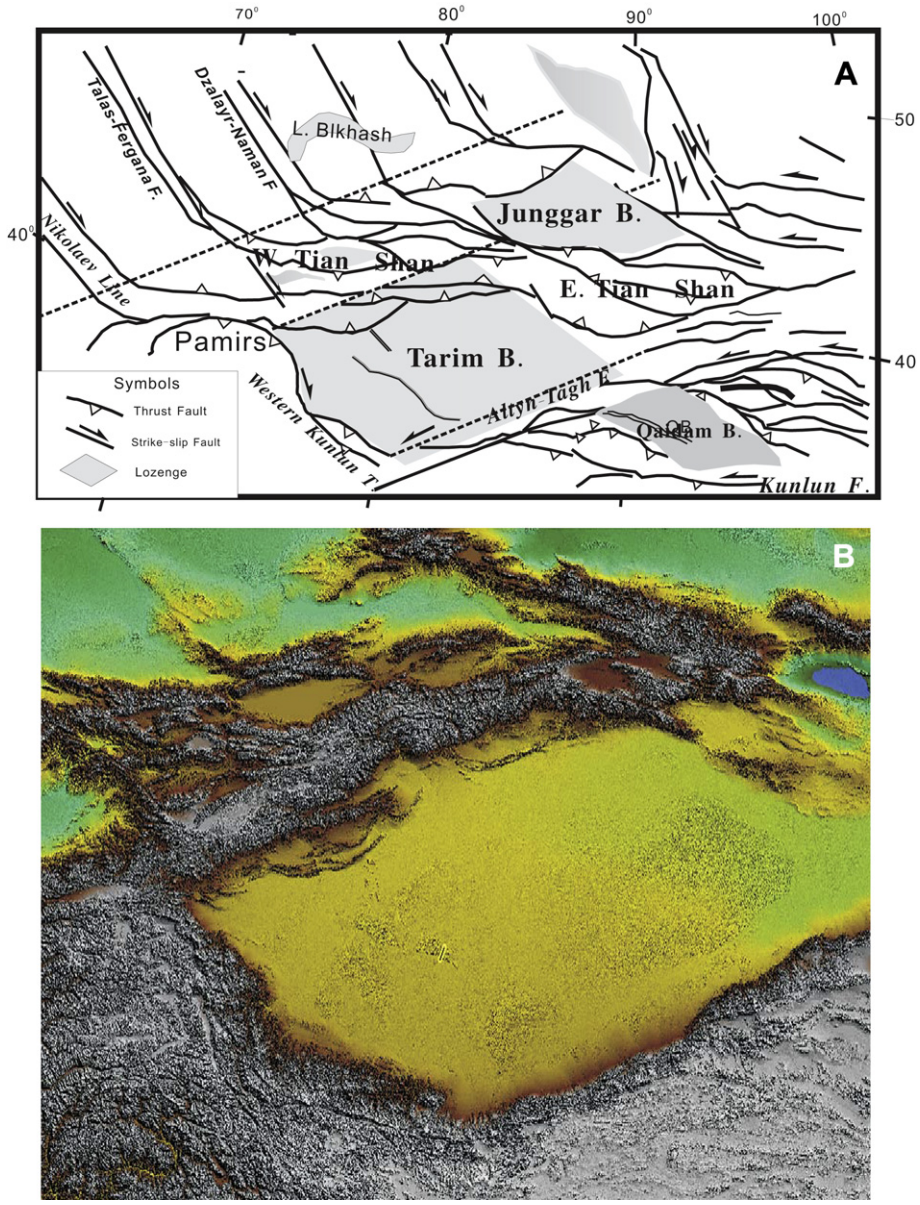

Fig. 5. Wide-open V-shaped conjugate strike-slip fault system in central Asia area: (A) Simplified geological map of central Asia; (B) Satellite photograph of central Asia. Source: Google Earth. The Altyn-Tagh fault formed early and controlled development in this broad area and formed the WNW-trending kink-bands in the Tarim and the Qaidam basins that are sub-parallel to the WNW-striking right-slip faults. The large −scale WNW-striking faults acted later and transformed the ENE-striking in the Keping and Kuche areas into a thrust belt which, in turn, truncated the 250-km-long Mazatagh kinkband (Fig. 6).

4. Major geological implications

The MEM criterion may provide a reasonable explanation for the following structures in nature whose origins are still puzzles in structural geology: (1) the obtuse angle in the contractional direction of conjugate kink-bands and extensional crenulation cleavages (eccs; Passchier and Trouw, 2005); (2) formation of low-angle normal faults, high-angle reverse faults and wide-open V-shaped conjugate fractures with anastomosing shear networks around lozenge blocks; (3) the criterion can be used to determine the stress state when the related deformation zones formed; (4) as discussed in detail below, it provides a approach to determine the vorticity number (W_k) when the related ductile shear features formed, because W_k can be derived from the orientation of the maximum principal stress (σ_1).

4.1. Conjugate angle of crenulation cleavage

A crenulation cleavage is a spaced cleavage that forms when an earlier foliation has been deflected into a new orientation, forming a series of straight-limb-dominant, small folds with narrow, tight curved hinges. There are two kinds of crenulation cleavages: (1) kink-bands (Price and Cosgrove, 1990) and contractional crenulation cleavages (cccs; Passchier and Trouw, 2005) that can form when contraction is parallel to the earlier foliation; (2) normal kink-bands (Price and Cosgrove, 1990) or extensional crenulation cleavages (eccs; e.g. Platt, 1979; Platt and Vissers, 1980; Passchier, 1991; Passchier and Trouw, 2005) that can form when contraction is normal to the foliation. The latter are also termed as shear bands that overprint the pre-existing mylonitic foliation (White, 1979; White et al., 1980; Carreras, 2001; Passchier and Trouw,

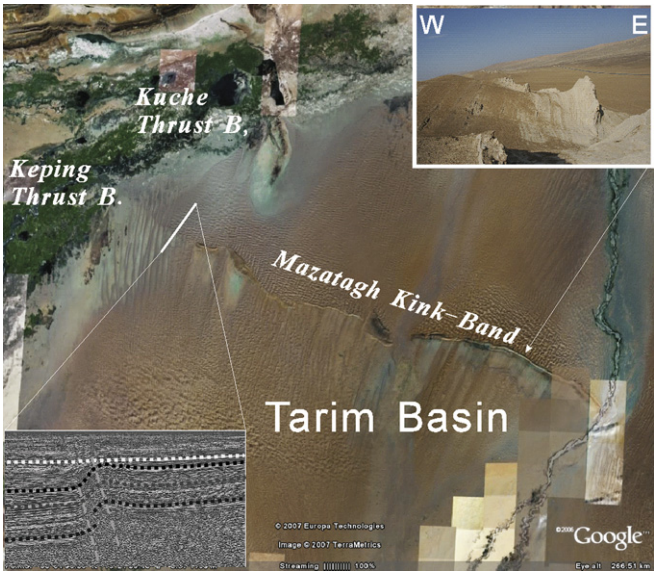

Fig. 6. The Mazatagh kinkband is over 250 km long and ~ 7 km wide in the Tarim Basin, China. Source: Google Earth. An outcrop and a seismic-profile of the kinkband are shown in right and left insets, respectively, showing the obvious high-angle south-dipping zone in the sub-horizontal field.

2005; Fusseis et al., 2006). They are generally synthetic and obtain the special term of C′ (Berthe et al., 1979) or S/C′-type shear bands (Passchier and Trouw, 2005).

The orientation of ecc has previously been suggested as representing either the inclined eigenvector during sub-simple shear flow (e.g., Bobyarchick, 1986; Pray et al., 1997), the direction of maximum rate of shear strain (e.g., Platt and Vissers, 1980; Simpson and De Paor, 1993) or the orientation of a Coulomb failure surface (Blenkinsop and Treloar, 1995).The first two theories require a stable homogeneous flow. It is difficult to apply them to crenulation cleavages, because crenulation cleavages occur as a result of deformation localization. There is also no positive evidence for the third theory; conjugate angles much larger than 60° do not support this model.

The conjugate angle of both cccs and eccs is usually ~110° and always in the direction of the σ_1 or the maximum shortening when a conjugate system forms. The conjugate angles of kink-bands observed in nature and experiments are from 101° to 130° and the conjugate angles of ecc system change from 95° to 120° (Zheng et al., 2004). As previously mentioned, the grey shadow area of Fig. 1 covers all the data available and the dark-grey shadow area covers all the data with a distinct yield stress provided by Gómez-Rivas (2008), and the four vertical lines represent the four conjugate angles measured by Kurz and Northrup (2008). The range of 55° ± 5° in Fig. 1 that is most favorable for crenulation cleavages to form demonstrates that the MEM-criterion controls the formation of crenulation cleavages.

4.2. Formation of low-angle normal faults or extensional detachment faults

Since the recognition of low-angle normal faults or extensional detachment faults in western North America in the early 1980's, their origin has been puzzling. This is because their occurrence is not compatible with the Mohr-Coulomb criterion and Anderson's predictions. Based on quantitative analysis of conjugate angles of eccs, Zheng et al. (2004) once noted, using the Yagan metamorphic core complex (mcc) in the Sino-Mongolian border areas as a case study, the striking similarity in geometry and kinematics between the ecc sets and low-angle normal faults on different scales. They argued that large-scale low-angle normal faults may originate in one of major eccs by strain localization and strain-softening. The low angular relationship between the Whipple detachment fault, California and the mylonitic front in its footwall (Davis and Lister, 1988) can be interpreted as an expression of the detachment fault propagating upward out of the mid-crustal mylonitic shear zone along a master ecc surface. In the Hohhot mcc of the Daqing Shan, Inner Mongolia, the Hohhot detachment fault is parallel to the synthetic ecc set in the footwall mylonitic rocks and the cut-off angle between the detachment fault and the mylonitic foliation is ~25–30° (Davis et al., 2002; Davis and Darby, 2010). This also implies the genetic relationship between the low-angle normal fault and the ecc set.

Field observations show that the Jinzhou fault in the Liaoning peninsular is an extensional detachment fault that is parallel to the C′-foliation in the underlying mylonitic rocks and truncates the penetrative mylonitic foliation (Zheng et al., 2009a,b; Fig. 4).

Lower plate C′ shear bands are parallel to the major detachment in the Betic Cordilleras, Spain and their density increases exponentially toward the contact. This demonstrates that the low-angle detachment was derived from a C′ shear band and resulted from a progressive localization of the deformation through time Agard et al., 2011).

4.3. Formation of high-angle reverses faults

According to the Mohr-Coulomb criterion and Anderson fault theory, reverse faults should dip at an angle less than 45°. High-angle reverse faults, however, are common in nature. Among famous examples are the high-angle reverse faults with gold-bearing quartz veins in Quebec province, Canada (Sibson et al., 1988; Boullier and Robert, 1992). The co-existence of high-angle ductile reverse faults and sub-horizontal extension fractures implies that the σ_1 and σ_2 were sub-horizontal and the σ_3 was sub-vertical when the faults and fractures formed. The attitude of the faults was not favorable for their reverse displacement due to high frictional resistance related to a high normal stress component on the fault-surfaces. Sibson et al. (1988) proposed the fault-valve model that has quite soundly elucidated the periodic activity along high-angle reverse faults in terms of periodic changes in fluid pressure. Although the model may resolve how movement on the fault-surface could occur, it does not resolve the origin of the high-angle reverse faults themselves. The MEM criterion can provide a reasonable explanation, because it predicts that the angle between ductile reverse faults is ~55° with a sub-horizontal principal stress axis in contractional regimes.

4.4. Lozenges and wide-open V-shaped conjugated ductile shear/fault zones

A special network consisting of anastomosing sub-vertical shear zones and lozenges, or unreformed or less deformed lozenges surrounded by anastomosing sub-vertical ductile-shear networks, are "especially abundant in continental crustal rocks, termed basement or 'crystallines'" (Ramsay and Huber, 1987). The dextral and sinistral sets of ductile shear zones form a conjugate system with an obtuse angle in the shortening direction (Ramsay and Graham, 1970; Mitra, 1979, 1998; Ramsay and Allison, 1979; Bell, 1981; Choukroune and Gapais, 1983; Gapais et al., 1987; Burg et al., 1996; Corsini et al., 1996; Czeck and Hudleston, 2003, 2004; Bhattacharyya and Czeck, 2008; Carreras et al., 2010). One example of wide-open V-shaped networks with lozenges is shown in Fig. 2D.

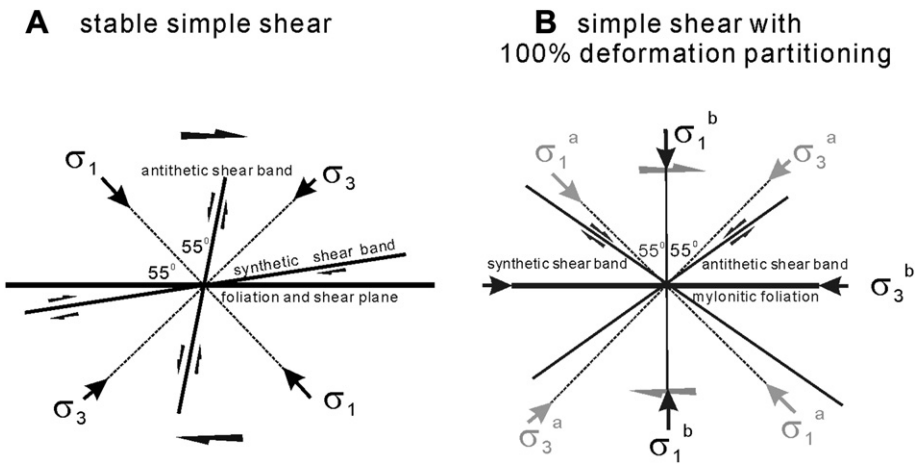

Fig. 7. Kinematic vorticity numbers (W_k) = sin2 × 45° = 1 for (A) the stable simple shear and W_k = sin2 × 0° = 0 for (B) the crenulation cleavage stage of the simple shear with 100% deformation partitioning: stress states for the mylonitic and crenulation stages shown as σ_1^a-σ_3^a and σ_1^b-σ_3^b, respectively.

Actually, lozenge structures are not only confined to basement or crystalline rocks. Taylor et al. (2003) showed that Cenozoic conjugate faults are widespread in central Tibet and found a series of V-shaped wedge blocks facing to the east, the extrusion direction suggested by Tapponnier and Molnar (1976, 1977). The so-called V-shaped conjugate faults have also been documented in the eastern Alps, western Turkey, eastern Afghanistan, western Mongolia, Southeast Asia, and Gulf of Thailand (Yin, 2010, and refs therein).

One of the common features of the V-shaped blocks is, as Yin pointed out, that they lie at 60–75° from the maximum compressive stress direction. According to our measurements, however, the angles range from 54° to 73.5° with an average of ~ 55.7° Zhang et al., 2010; Zheng et al., 2011; e.g. Fig. 5), which is very close to the prediction of the MEM criterion.

Experimental data show that not all individual shears are simultaneously active (Williams and Price, 1990; Mancktelow, 2002). It is also the case in Central Asia. The ENE-striking left-slip Altyn-Tagh fault and WNW-striking right-slip faults have both deformed the Pliocene strata in Central Asia. However, the Altyn-Tagh fault was active early (Meng et al., 2001) and controlled this area so that caused the formation of WNW-trend kink-bands in the Tarim and the Qaidam basins that are sub-parallel to the WNW-trend right-slip faults (Zheng et al., 2007, 2011; Figs. 4 and 6). Later, the WNW-trend right-slip faults were active and reformed the northwestern boundary fault of the Tarim Basin into transpressional zone (the Keping thrust belt and Kuche thrust belt) that, in turns, truncated the 250- km-long Mazatagh kinkband that may be rated as a *giant* in kink-bands (Fig. 6).

4.5. C′-method estimating kinematic vorticity number (W_k)

Bobyarchick (1986) defined W_k in the simplest way as the cosine of the angle α between the eigenvectors or apophyses:

$$W_k = \cos\ \alpha \tag{2}$$

According to the definition, $W_k = 0$ for pure shear zones, $W_k = 1$ for simple shear zones and W_k of general shear zones ranges in between.

Three main analytical techniques are broadly grouped into those that use tailed and tailless porphyroclasts to estimate W_k in high strain zones (Passchier, 1987; Simpson and De Paor, 1993, 1997; Wallis, 1992, 1995). All of which are on the same fundamental mathematical relationships between W_k, R or shape factor (B^*) and the angle of porphyroclast long axes with respect to foliation (θ). Jessup et al. (2007) unified these methods and proposed the Rigid Grain Net (RGN) method.

W_k can also be given by

$$W_k = \sin\ 2\xi \tag{3}$$

(Weijermars, 1991, 1993, 1998) where ξ is the angle between σ_1 and the normal to the shear zone. Since shear bands are theoretically and practically confirmed at an angle of ~55° with the major principal stress axis (σ_1), they can, therefore, serve as a new reliable quantitative vorticity indicators. W_k values inferred from shear bands are not necessarily consistent with those from porphyroclast hyperbolic distribution (PHD) analysis (Simpson and De Paor, 1997). The numerical modeling to investigate the reliability of the widely used PHD method (Li and Jiang, 2011) shows that the vorticity numbers between 0.5 and 0.85 reported from natural shear zones in the literature using PHD method could all have been produced in zones with close-to-simple-shearing flow. The angle between the synthetic ecc and C′ and the mylonitic foliation proposed by various authors generally ranges from 15 to 35° (Passchier and Trouw, 2005). The vorticity numbers estimated in terms of C′ and based on Eq. (3) would range from 0.64 to 0.00, much less than their PHD counterparts. As shown in Fig. 7, $W_k = 1$ for a stable simple shear flow, while $W_k = 1$ for the mylonitic stage and $W_k = 0$ for the crenulation cleavage stage of a simple shear with 100% deformation partitioning during progressive deformation. Abortion of simple shear component must decrease the W_k in the shear zone (Zheng et al., 2009a,b).

5. Discussion and conclusions

Since the intersection angle of ~110° widely appears in materials from low yield strengths such as argillaceous sediments, evaporites and fault-gouges to combination of various rocks and in the case of crystalline materials involved, it seems to disregard the orientations of crystal lattice (e.g. quartz in Fig. 2A, mica in Fig. 2B) and cordierite reported by Kruhl et al. (2007), it may be regarded as a quasi-material-invariant. In addition, because the angle is observed on scales from 10^6 m (e.g. Fig. 5) to 10^{-7} m (e.g. Fig. 2E); it may also be rated as scale-invariant, or at least, as quasi-invariant.

The MEM criterion is widely applicable to localized deformation in ductile materials and such localization, as Hubert-Ferrari et al. (2003) and Gómez-Rivas (2008) suggested, can be regarded as a competing process between an external loading rate and the rate of viscous relaxation of the material. If the former is higher than the latter, there will be an increasing differential stress until the yield point is reached.

Ductile shear features will nucleate and propagate afterward, and become an anastomosing shear network. Alternatively, if the viscous rate is able to relax the imposed stress, ductile shear fractures will not nucleate and the deformation will be distributed homogeneous or heterogeneously within the material. The limit in between therefore constitutes the ductile/brittle transition that is crucial to understand the rock behavior in the continental lithosphere.

The depth of 10–15 km is usually regarded as a brittle/ductile transition zone for felsic rocks with mylonitic tectonites as the common products of deformation immediately below this zone. However, a number of the conjugate-intersection angle of ~110° that are closely related to ductile deformation described in Section 3 obviously occurred on shallow levels without any metamorphism as shown in Fig. 2C, E, G, H, Figs. 3A and 4A, B. Mylonitic rocks with a certain metamorphism are therefore not a unique indicator of ductile behavior. What else can be served as a marker of ductile deformation? The essential difference between brittle- and ductile-fracturing depends on how large a strain the material is able to sustain before fracturing or faulting. A rule-of-thumb holds that fractures that occurred at less than 3–5% strain are regarded as brittle-fractures and those that occurred at more than 5–10% strain indicate ductile-fracturing. Therefore, brittle fracturing belongs to the category of elastic or small-strain deformation in which the factor of time is not considered. Ductile-fracturing, on the other hand, belongs to the category of large-strain deformation in which the strain is closely depended on the factor of time that must be considered. If a given rock was located at a shallow level with low *P–T* conditions under which no metamorphism happened, only at a certain low strain-rate may the rock show ductile behavior. In this respect, rock-behavior is quite similar to a ball of 'bouncing or silly putty', which will bounce elastically if you let it fall down to the floor, or to the contrary, when you place it on a table, it will exhibit plastic behavior and become pancake-shaped in one or 2 h.

Large-strain localized deformation is, therefore, a reliable marker of ductile-fracturing. If a distinct deflection or "drag-fold" is adjacent to a fault, the fault is probably a ductile one, because less than 5–10% strain is usually invisible. Although the fault-gouge is commonly regarded as a result of brittle-fracturing at shallow levels (e.g. Sibson, 1977), S/C fabrics in fault-gouge zones as shown in Fig. 2G imply that the behavior of gouge itself was similar to ductile flow of mylonitic rocks.

Kinkbands of phyllite were produced experimentally at room temperature and the strain-rate of $4–8 \times 10^{-4} s^{-1}$ by Paterson and Weiss (1966). Although most of their experiments were run a at 5 kb confining pressure that corresponds to the pressure at a depth of 16–17 km, the stress-strain curves at different (lower) confining pressures show that the yield-strength at 1 kb confining pressure is about half that at 5 kb confining pressure (Fig. 5 of Paterson and Weiss, 1966); their brass-jacketed specimens deformed at 1 and 2.5 kb also showed kinking. These results confirm that large-strain deformation of phyllite can occur at room temperature and at a strain-rate of 10^{-4} s^{-1}, which is ~10 indices higher than the 'standard geological strain-rate' of 10^{-14} s^{-1}(e.g. Twiss and Moores, 2007).

From the cases described and the above-discussions the following conclusions can be drawn: 1) the MEM-criterion derived from mechanic analysis is based on empirical data that come from both experiments and naturally deformed samples; 2) no matter what a material is involved, homo- or heterogeneous, isotropic or anisotropic, even disregarding the crystallographic lattice, the conjugate angle of ductile fractures containing the principal compressive axis (σ_1) is obtuse, typically, 109° or 110° and this is a quasi-invariant probably for the scale-range of 10^{-7}–10^{6} m; 3) brittle-fractures mainly occurred at, but were not confined to shallow levels and ductile fractures mainly developed at, but not confined to deep levels. Rock-behavior, similar to a ball of "bouncing putty", may show elastic behavior at high strain-rates and plastic behavior at low strain-rates.

Acknowledgments

This work was funded by NNSFC (Grant No. 90714006 and No. 40872133). We thank Professors Laurel Goodwin and Basil Tikoff for their comments on the manuscript of *Challenge to slip-lines in extrusion tectonics* that is rejected and for suggesting that we should write a synthesis of the MEM Criterion. Special thanks to an anonymous reviewer #2 for recommending an unpublished thesis by Gomez Rivas, whose excellent simulations provide solid evidence that the 109 or 110° is a material-invariant. Finally, Yadong is indebted to Greg Davis and Yin An for their long term help both in science and language!

References

Agard, P., Augier, R., Monie, P., 2011. Shear band formation and strain localization on a regional scale: evidence from anisotropic rocks below a major detachment (Betic Cordilleras, Spain). Journal of Structural Geology 33, 114–131.
Anderson, E.M., 1951. The Dynamics of Faulting, second ed. Oliver and Boyd Edinburgh.
Anderson, T.B., 1964. Kink-band and related geological structures. Nature 202, 272–274.
Becker, G.F., 1893. Finite homogeneous strain, flow and rupture of rocks. Geological Society of America Bulletin 4, 13–19.
Bell, T.H., 1981. Foliation development: the contribution, geometry and significance of progressive, bulk, inhomogeneous shortening. Tectonophysics 75, 273–296.
Berthe, D., Choukroune, P., Jegouzo, P., 1979. Orthogneiss, mylonite, and noncoaxial deformation of granite: the example of the South Armorican shear zone. Journal of Structural Geology 2, 31–42.
Bhattacharyya, P., Czeck, D.M., 2008. Using network analyses within GIS technologies to quantify geometries of shear zone networks. Geosphere 2, 640–656.
Blenkinsop, T.G., Treloar, P.L., 1995. Geometry, classification and kinematics of S-C fabrics. Journal of Structural Geology 17, 397–408.
Bobyarchick, A.R., 1986. The eigenvalues of steady state flow in Mohr space. Tectonophysics 122, 35–51.
Boullier, A–M, Robert, F., 1992. Palaeoseismic events recorded in Archaean gold-quartz vein networks, Val d'Or, Abitibi, Quebec, Canada. Journal of Structural Geology 14, 161–179.
Burg, J.-P., Ricou, L.-E., Ivanov, Z., Godfriaus, I., Dimov, D., Klain, L., 1996. Syn-metamorphic nappe complex in the Rhodope massif. Structure and Kinematics Terra Nova 8, 6–15.
Carreras, J., 2001. Zooming on northern Cap de Creus shear zones. Journal of Structural Geology 23, 1457–1486.
Carreras, J., Czeck, D.M., Druuet, E., 2010. Structure and development of an anastomosing network of ductile shear zones. Journal of Structural Geology 32, 656–666.
Carreras, J., Druguet, E., Griera, A., Soldevila, J., 2004. Strain and deformation history in a syntectonic pluton. The case of the Roses granodiorite (Cap de Creus, Eastern Pyrenees). In: Alsop, G.I., Holdsworth, R.E., McCaffrey, K.J.W., Hand, W. (Eds.), Flow Process in Faults and Shear Zones. The Geological Society, London, Special Publications, vol. 224, 370–319.
Choukroune, P., Gapais, D., 1983. Strain pattern in the Aar granite (Central Alps): orthogneiss developed by bulk inhomogeneous flattening. Journal of Structural Geology 5, 411–418.
Corsini, M., Vauchez, A., Caby, R., 1996. Ductile duplexing at a bend of a continental-scale strike-slip shear zone: example from NE Brazil. Journal of Structural Geology 18, 385–394.
Czeck, D.M., Hudleston, P.J., 2003. Testing models for obliquely plunging lineations in transpression: a natural example and theoretical discussion. Journal of Structural Geology 25, 959–982.
Czeck, D.M., Hudleston, P.J., 2004. Physical experiment of vertical transpression with localized nonvertical extrusion. Journal of Structural Geology 26, 573–581.
Davis, G.A., Darby, B.J., Zheng, Y., Spell, T.L., 2002. Geometric and temporal evolution of an extensional detachment fault, Hohhot metamorphic core complex, Inner Mongolia, China. Geology 30, 1993–1006.
Davis, G.A., Darby, B.J., 2010. Early Cretaceous overprinting of the Mesozoic Daqing Shan fold-and-thrust belt by the Hohhot metamorphic core complex, Inner Mongolia, China. Geoscience Frontiers 1, 1–20.
Davis, G.A., Lister, G.S., 1988. Detachment faulting in continental extension: perspectives from the southwestern U.S. Cordillera. Geological Society of America Special Paper 218, 133–159.
Davis, G.A., Qian, X., Zheng, Y., Tong, H., Yu, H., Wang, C., Gehrels, G.E., Shanfiquallah, M., Fryxell, J.E., 1996. Mesozoic deformation and plutonism in the Yunmeng Shan: a Chinese metamorphic core complex north of Beijing, China. In: Yin, A., Harrison, T.M. (Eds.), The Tectonic Evolution of Asia. Cambridge University Press, pp. 253–280.

Fowler, A., Osman, A.F., 2009. The Sha'it-Nugrus Shear zone separating central and south eastern deserts, Egypt: a post-arc collision low-angle normal ductile shear zone. Journal of African Earth Sciences 52, 16–32.
Fusseis, F., Handy, M.R., Schrank, C., 2006. Networking of shear zones at the brittle-to viscous transition (Cap de Creus, NE Spain). Journal of Structural Geology 28, 1228–1243.
Gapais, D., Bale, P., Choukroune, P., Cobbold, P.R., Mahjoub, Y., Marquer, D., 1987. Bulk kinematics from shear zone pattern: some field examples. Journal of Structural Geology 8, 635–646.
Gómez-Rivas, E., 2008. Localización de deformación en medios dúctiles y anisótropos: studio de campo, experimental y numérico, Tesis doctoral. Universitat Autònoma de Barceloma. http://www.tesisenxarxa.net/TDX-1120108-151236.
Guo, Z.J., Shi, H.Y., Zhang, Z.C., Zhang, J.J., 2006. The tectonic evolution of south Tianshan paleo-oceanic crust inferred from the spreading structures and Ar–Ar dating of the Hongliuhe ophiolites, NW China. Acta Petrologica Sinica 22, 95–102.
Hill, R., 1950. The Mathematical Theory of Plasticity. Oxford University Press/ Clarendon Press, Oxford.
Hubert-Ferrari, A., King, G., Manighetti, I., Aomijo, R., Meyer, B., Tapponnier, P., 2003. Long-term elasticity in the continental lithosphere: modeling the Aden Ridge propagation and the Anatolian extrusion process. Geophysical Journal International 153, 111–132.
Jessup, M.J., Law, R.D., Frassi, C., 2007. The Rigid Net (RGN): an alternative method for estimating mean kinematic vorticity number (W_m). Journal of Structural Geology 29, 411–421.
King, D.C., Klepeis, K.A., Goldstein, A.G., Gehrels, G.E., Clarke, G., 2008. The initiation and evolution of the transpressional Straight River shear zone, central Fiordland, New Zealand. Journal of Structural Geology 30, 410–430.
Kruhl, J.H., et al., 2007. Brittle–ductile microfabrics in natural deformed cordierite: evidence for significant short-term variations. Journal of Structural Geology 29, 355–374.
Kurz, G.A., Northrup, C.J., 2008. Structural analysis of mylonitic rocks in the Cougar Creek Complex, Oregon-Idaho using the porphyroclast hyperbolic distribution method, and potential use of SC'-type extensional shear bands as quantitative vorticity indicators. Journal of Structural Geology 30, 1005–1012.
Li, C., Jiang, D., 2011. A critique of vorticity analysis using rigid clasts. Journal of Structural Geology 33, 203–219.
Lin, A., Ren, Z., Kumahara, R., 2010. Structural analysis of coseismic shear zone of the 2008 M_w 7.9 Wenchuan earthquake, China. Journal of Structural Geology 32, 781–791.
Mancktelow, N.S., 2002. Finite-element modeling of shear zone development in viscoelastic materials and its implications for localization of partial melts. Journal of Structural Geology 24, 1045–1053.
Marshak, S., Alkmim, F.F., Whittington, A., Pdrosa-Soares, A.C., 2006. Extensional collapse in the Neoproterozoic Aracuai orogen, eastern Brazil: a setting for reactivation of asymmetric crenulation cleavage. Journal of Structural Geology 28, 129–147.
Meng, Q.R., Hu, J.M., Yang, F.Z., 2001. Timing and magnitude of displacement on the Altyn Tagh fault: constraints from stratigraphic correlation of adjoining Tarim and Qaidam basins, NW China. Terra Nova 13, 86–91.
Mitra, G., 1979. Ductile deformation zones in Blue Ridge basement rocks and estimation of finite strain. Geological Society of America Bulletin 90, 935–951.
Mitra, G., 1998. Anastomosing deformation zones. In: Snoke, A.W., Tullis, J., Todd, V.R. (Eds.), Fault-Related Rocks: A Photographic Atlas. Princeton University Press, pp. 142–143.
Neves, S.P., de Silva, J.M.R., Mariano, G., 2005. Oblique lineations in orthogneisses and supracrustal rocks: vertical partitioning of strain in a hot crust (eastern Borborema Province, NE Brazil). Journal of Structural Geology 27, 1513–1527.
Odonne, F., Massonnat, G., 1992. Volume loss and deformation around conjugate fractures: comparison between a natural example and analog experiments. Journal of Structural Geology 14, 963–972.
Park, R.G., 1981. Shear-zone deformation and bulk strain in granite-greenstone terrain of the Western Superior Province, Canada. Precambrian Research 14, 31–47.
Passchier, C.W., 1987. Stable positions of rigid objects in non-coaxial flow- a study in vorticity analysis. Journal of Structural Geology 9, 679–690.
Passchier, C.W., 1991. Geometric constrains on the development of shear bands in rocks. Geplogie en Mijnbpuw 70, 203–211.
Passchier, C.W., Trouw, R.A.J., 2005. Microtectonics, second ed. Springer-Verlag, Berlin. 366pp.
Paterson, M.S., Weiss, L.E., 1966. Experimental deformation and folding in phyllite. Geological Society of America Bulletin 77, 343–374.
Peacock, D.C.P., 1991. Displacement and segment linkage in strike-slip fault zones. Journal of Structural Geology 13, 1025–1035.
Peltzer, G., Tapponnier, P., 1988. Formation and evolution of strike-slip faults, rifts, and basins during India-Asia collision: an experimental approach. Journal of Geophysical Research 93, 85–117.
Platt, J.P., 1979. Extensional crenulation cleavage. Journal of Structural Geology 1, 95–96.
Platt, J.P., Vissers, R.L.M., 1980. Extensional structures in the anisotropic rocks. Journal of Structural Geology 2, 397–410.
Pray, J.R., Secor Jr., D.T., Maher Jr., H.D., 1997. Rotation of fabric elements in convergent shear zones, with examples from the southern Appalachians. Journal of Structural Geology 19, 1023–1036.
Price, N.J., Cosgrove, J.W., 1990. Analysis of Geological Structures. Cambridge University Press, Cambridge, UK. 502pp.
Ramsay, J.G., 1980. Shear zone geometry: a review. Journal of Structural Geology 2, 83–99.
Ramsay, J.G., Allison, L., 1979. Structural analysis of shear zones in an Alpinised Hercynian granite, Maggia Nappen, Pennine zone, Central Alps. Schweizer Mineralogische und Petrographische Mitteilungen 59, 251–279.
Ramsay, J.G., Graham, R./H./, 1970. Strain variations in shear belts. Canadian Journal of Earth Sciences 7, 786–813.
Ramsay, J.G., Huber, M.I., 1987. The Techniques of Modern Structural Geology Fractures. In: Folds and Fractures, vol. 2. Academic Press, New York.
Sibson, R.H., 1977. Fault rocks and fault mechanisms. Journal of the Geological Society of London 133, 191–213.
Simpson, C., De Paor, D.G., 1993. Strain and kinematic analysis in general shear zones. Journal of Structural Geology 15, 1–20.
Simpson, C., De Paor, D.G., 1997. Practical analysis of general shear zones using porphyroclasts hyperbolic distribution method: an example from the Scandinavian Caledonides. In: Sengupta, S. (Ed.), Revolution of Geological Structures in Micro- to Macro-scales. Chapman and Hall, London, pp. 169–184.
Sibson, R.H., Robert, F., Poulsen, K.H., 1988. High-angle reverse faults, fluid-pressure cycling, and mesothermal gold-quartz deposits. Geology 16, 551–554.
Sun, Y., Shu, L., Lu, X., Liu, H., Zhang, X., Lin, A., Kosaka, K., 2008. Recent progress in studies on the nano-sized particle layer in rock shear planes. Progress in Natural Science 18, 367–373.
Tapponnier, P., Molnar, P., 1976. Slip-line field theory and large-scale continental tectonics. Nature 264, 319–324.
Tapponnier, P., Molnar, P., 1977. Active faulting and tectonics in China. Journal of Geophysical Research 82, 2905–2930.
Tapponnier, P., Peltzer, G., Le Dain, A.Y., Armijo, R., Cobbold, P., 1982. Propagating extrusion tectonics in Asia: new insights from simple experiments with plasticine. Geology 10, 611–616.
Taylor, M., Yin, A., Ryerson, F.J., Kapp, P., Ding, L., 2003. Conjugate strike-slip faulting along the Bango-Nujiang suture zone accommodates coeval east–west extension and north–south shortening in the interior of the Tibet plateau. Tectonics 22, 1044. doi:10.1029/2002TC001361.
Twiss, R.J., Moores, E.M., 2007. Structural Geology. W.H. Freeman and Company, New York. 736.
Ujiie, K., Malman, A.J., Sanchez-Gomez, M., 2004. Origin of deformation bands in argillaceous sediments at the toe of the Nankai accretionary prism, southwest Japan. Journal of Structural Geology 26, 221–321.
Vernooij, M.G.C., Kunze, K., den Brok, B., 2006. 'Brittle' shear zones in experimentally deformed quartz single crystals. Journal of Structural Geology 28, 1292–1306.
Watterson, J., 1999. The future of failure: stress or strain? Journal of Structural Geology 21, 939–948.
Wernicke, B., 1981. Low-angle normal faults in the Basin and Range Province: nappe tectonics in an extending orogen. Nature 291, 645–646.
Weijermars, R., 1991. The role of stress in ductile deformation. Journal of Structural Geology 13, 1061–1078.
Weijermars, R., 1993. Progressive deformation of single layers under constantly oriented boundary stresses. Journal of Structural Geology 15, 911–922.
Weijermars, R., 1998. Taylor-mill analogues for patterns of flow and deformation in rocks. Journal of Structural Geology 20, 77–92.
Wallis, S.R., 1992. Vorticity analysis in a metachert from the Sanbagawa belt, SW Japan. Journal of Structural Geology 14, 271–280.
Wallis, S.R., 1995. Vorticity analysis and recognition of ductile deformation in the Sanbagawa Belt, SW Japan. Journal of Structural Geology 17, 1077–1093.
Wang, X.S., Zheng, Y.D., Wang, T., 2007. Strain and shear types of the Louzidian shear zone in southern Chifeng, Inner Mongolia, China. Science in China, Series D, 50487–50495.
White, S.H., 1979. Large strain deformation: report on a tectonic studies Group discussion meeting held at Imperial College, London on 14 November 1979. Journal of Structural Geology 1, 333–339.
White, S.H., Burrows, S.E., Carreras, J., Shaw, N.D., Humphteys, F.J., 1980. On mylonites and ductile shear zones. Journal of Structural Geology 2, 175–187.
Williams, P.F., Price, G.P., 1990. Origin of kinkbands and shear-band cleavage in shear zones: an experimental study. Journal of Structural Geology 12, 145–164.
Yang, T.N., Wang, Y., Li, J.Y., Sun, G.H., 2007. Vertical and horizontal strain partitioning of the central Tianshan (NW China) evidence from structures and $^{40}Ar/^{39}Ar$ geochronology. Journal of Structural Geology 29, 1605–1621.
Yin, A., 2010. Cenozoic tectonic evolution of Asia: a preliminary synthesis. Tectonophysics 488, 293–325.
Yin, A., Taylor, M.H., Mechanics of V-shaped conjugate strike-slip faults and the corresponding continuum mode of continental deformation. Geological Society of America Bulletin, in press, doi:10.1130/B30159.1.
Zhang, B., Zhang, J.J., Zhong, D., 2010. Structure, kinematics and ages of transpression during strain-partitioning in the Chongshan shear zone, western Yunnan, China. Journal of Structural Geology 32, 445–463.
Zheng, Y.D., Mo, W.L., Zhang, W.T., Guan, P., 2007. A new idea for petroleum exploration in the Chaidamu Basin. Petroleum Exploration and Development 34, 13–18 (In Chinese with an English abstract).
Zheng, Y.D., Wang, E., Zhang, J.J., Wang, T., 2011. A challenge to the concept of slip-lines in extrusion tectonics. Geoscience Frontiers 2, 23–34.
Zheng, Y.D., Wang, T., Ma, M., Davis, G.A., 2004. Maximum effective moment criterion and the origin of low-angle normal faults. Journal of Structural Geology 26, 271–285.

Zheng, Y.D., Wang, T., Wang, X.S., 2006. The maximum effective moment criterion (MEMC) and its implications in structural geology. Acta Geologica Sinica 80, 70–78.
Zheng, Y.D., Wang, T., Zhang, J.J., 2009a. Comment on "Structural analysis of mylonitic rocks in the Cougar Creek Complex, Oregon-Idaho using the porphyroclast hyperbolic distribution method, and potential use of SC'-type extensional shear bands as quantitative vorticity indicators". Journal of Structural Geology 31, 541–543.
Zheng, Y.D., Zeng, L.S., Li, J.B., Ouyang, Z.X., 2009b. Mesozoic orogenic-contractional decollement and late-orogenic extensional in the southern Liaoning Peninsula. Chinese Journal of Geology 44, 811–824 (In Chinese with an English abstract).